Response Characteristics and Mathematical Modeling for a Nitric Oxide Fiber-Optic Chemical Sensor

ARTICLE *in* ANALYTICAL CHEMISTRY · MAY 1996

Impact Factor: 5.64 · DOI: 10.1021/ac951224g

2 AUTHORS, INCLUDING:

George Zhou
Merck

44 PUBLICATIONS **883** CITATIONS

SEE PROFILE

Anal. Chem. **1996,** *68,* 1748−1754

Response Characteristics and Mathematical Modeling for a Nitric Oxide Fiber-Optic Chemical Sensor

Xiangji Zhou and Mark A. Arnold*

Department of Chemistry, University of Iowa, Iowa City, Iowa 52242

A novel fiber-optic sensor for nitric oxide is constructed by holding a small amount of an internal reagent solution at the tip of a fiber-optic bundle with a piece of gas-permeable membrane. Nitric oxide diffuses across the membrane into this internal solution, where a chemiluminescent reaction between nitric oxide, hydrogen peroxide, and luminol takes place. The resulting light intensity is related to the concentration of nitric oxide in the sample. Results are presented from experiments to optimize the magnitude and rate of the sensor response. The resulting sensor possesses a limit of detection of 1.3 μM, a response time of 8−17 s, and a dynamic range from 5 to 40 μM. A mathematical model is derived to explain the sensor response as a function of time. Oxidation of nitric oxide by ambient oxygen and mass transport of nitric oxide through the gas-permeable membrane are considered in this model. The excellent agreement between experimental data and model predictions indicates that the oxidation of nitric oxide by oxygen is a major factor in this measurement, regardless of transducer element. The model further indicates a reaction rate constant for the oxygen oxidation of nitric oxide of $9.5(\pm 0.5) \times 10^6$ M^{-2} s^{-1} and a diffusion coefficient for nitric oxide in the silicone membrane of $5.0(\pm 0.2) \times 10^{-11}$ m^2 s^{-1} at 30 °C.

Nitric oxide is thought to play critical roles in numerous physiological and biological processes.[1] As a result, accurate measurements of nitric oxide in complex biological matrixes are needed to unravel the actions of this important compound. Two methods are commonly used for nitric oxide measurements. The first involves reaction with ozone, followed by chemiluminescence (CL) detection.[2,3] The second is based on the conversion of oxyhemoglobin to methemoglobin upon reaction with nitric oxide, followed by a subsequent absorbance measurement.[4,5] In addition, an amperometric sensor has been proposed recently based on a porphyrinic-catalyzed oxidation reaction.[6] This electrochemical approach requires a high operating potential (≥630 mV), which may render the measurement subject to interference by easily oxidized endogenous compounds. All three measurement schemes are complicated by the rapid oxidation of nitric oxide by ambient oxygen in aqueous media.[1]

A novel CL sensing scheme has been demonstrated by Kikuchi and co-workers.[7] In this system, nitric oxide is oxidized by hydrogen peroxide to form peroxynitrous acid (ONOOH), which subsequently reacts with luminol to form a photon via a CL process. A flow system was constructed by these researchers to measure nitric oxide released from intact kidney tissue. Released nitric oxide was captured in a perfusion buffer, which then served as a carrier stream for the on-line measurement of nitric oxide.

In this work, a new fiber-optic chemical sensor (FOCS) is proposed for nitric oxide based on this nitric oxide−hydrogen peroxide−luminol CL reaction scheme. Figure 1 shows the various phases and reactions associated with this sensor design. Nitric oxide from the sample diffuses across a gas-permeable silicone membrane and enters an internal solution composed of hydrogen peroxide and luminol. Under appropriate conditions, the entering nitric oxide reacts immediately with hydrogen peroxide to form the strong oxidant peroxynitrite, which then quickly reacts with luminol to generate light. A fiber-optic probe collects a fraction of the produced photons and directs this light to a photomultiplier tube (PMT) for detection. The resulting signal is related to the concentration of nitric oxide in the sample solution.

In this paper, the experimental parameters affecting the overall response properties of this nitric oxide FOCS are established. The corresponding optimum conditions are identified, and the resulting analytical response properties are reported. In addition, a mathematical model is derived to explain the time-dependent response of this sensor in the absence and presence of ambient oxygen.

EXPERIMENTAL SECTION

Materials. Hydrogen peroxide (30% solution), L-cysteine, dopamine, sodium hydrosulfite, Sephadex G-25, and hemoglobin (bovine, double crystallized, dialyzed, and lyophilized) were purchased from Sigma Chemical Co. (St. Louis, MO). Nitric oxide (gas 99.5%) was obtained from Matheson Gas Products (Twinsburg, OH). Sodium tetraborate decahydrate and pyrogallol were from Aldrich Chemical Co., Inc. (Milwaukee, WI). Sodium pyrophosphate was supplied by EM Science (Cherry Hill, NJ). All other chemicals were reagent grade quality obtained from common suppliers. Microporous Teflon membranes were purchased from Gore & Associates (Elkton, MD). Nonvulcanized

(1) Feldman, P. L.; Griffith, O. W.; Stuehr, D. J. *Chem. Eng. News* **1993**, December 20, 26−38.
(2) Bates, J. N. *NeuroProtocols* **1992**, *1* (2 October), 141−149.
(3) Palmer, R. M. J.; Ferrige, A. G.; Moncada, A. *Nature (London)* **1987**, *327*, 524−526.
(4) Balcioglu, A.; Maher, T. J. *J. Neurochem.* **1993**, *61* (6), 2311−2313.
(5) Kelm, M.; Schrader, J. *J. Circ. Res.* **1990**, *66*, 1561−1575.
(6) Malinski, T.; Taha, Z. *Nature (London)* **1992**, *358*, 676−678.
(7) Kikuchi, K.; Nagano, T.; Hayakawa, H.; Hirata, Y.; Hirabe, M. *Anal. Chem.* **1993**, *65*, 1794−1799.

S0003-2700(95)01224-8 CCC: $12.00

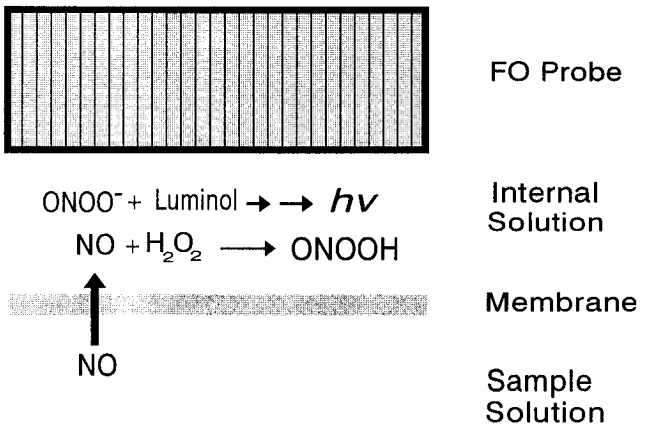

Figure 1. Membrane phases and reaction chemistry for the nitric oxide fiber-optic sensor.

matte-matte silicone sheets (0.051 and 0.127 mm thicknesses) were obtained from Specialty Manufacturing Inc. (Hemlock, MI).

All aqueous solutions were prepared in deionized water purified with a Milli-Q reagent water system (Millipore, Bedford, MA). Hydrogen peroxide solutions were standardized by titration with thiosulfate.[9]

Preparation of Nitric Oxide Stock Solutions. Stock solutions of nitric oxide were prepared according to the following procedure.[5,11] Deionized water underwent an ultrasonic treatment for at least 10 min, followed by a 60 min bubbling with purified argon. This argon gas had been previously passed through an alkaline pyrogallol (5% w/v) solution to scavenge traces of oxygen. Nitric oxide stock solutions were prepared by bubbling purified nitric oxide gas through the treated water for a minimum of 10 min. NO gas was purified by passing through solutions of 5% (w/v) pyrogallol in saturated potassium hydroxide and 10% (w/v) potassium hydroxide to remove other nitrogen oxides. The concentration of nitric oxide in the resulting stock solution was constant for more than 6 months when stored at 5 °C.[11]

Nitric oxide stock solutions were standardized by the photometric method based on the conversion of oxyhemoglobin to methemoglobin.[5,10,12] Oxyhemoglobin was prepared according to standard literature procedures.[5,10] Absorbance measurements were performed with a modified Cary-14 spectrometer (OLIS, Bogart, GA).

Chemiluminescence Measurements. All CL measurements for optimizing the internal solution composition were made with a SLM-Amino SPF-500C spectrofluorometer operating with the source off. The emission monochromator was set at 425 nm with a band pass of 20 nm. Voltage of the photomultiplier was set at 800 V, and the detector gain was set at 100. The following procedure was used to monitor the CL reaction. To begin, 2.05 mL of buffer containing hydrogen peroxide and luminol was placed in a typical 1 × 1 cm^2 fluorescence cell. Argon gas was continually passed over this solution once positioned in the spectrometer. The CL signal was monitored as a function of time as the appropriate amount of nitric oxide was injected with a standard gas-tight glass syringe (Hamilton Co., Reno, NV).

Sensor Construction. FOCSs for nitric oxide were made according to the schematic diagram in Figure 1. A gas-permeable membrane was used to hold an internal solution on the tip of a fiber-optic bundle. The membrane was stretched over the opening of a plastic tube and then held in position with an O-ring. Approximately 150 μL of the internal enzyme solution was then placed on top of the membrane, and the fiber-optic bundle was positioned within the plastic tube. The inner diameter of the plastic tube was 6 mm, while the diameter of the exposed portion of the membrane was 5 mm. The fiber-optic bundle had an outer diameter of 3 mm, and, when fully constructed, the fiber-optic bundle just touched the top of the internal solution. The internal solution was composed of hydrogen peroxide, luminol, and buffer at a specified pH. CL light was collected with the same setup as reported elsewhere.[9]

Sensor Measurements. Response of the fiber-optic nitric oxide sensor was measured by immersing the sensor tip in a 2.5 mL aliquot of a 0.05 M phosphate buffer set at pH 7.4. The buffer was stirred continuously with a magnetic bar, and the solution temperature was maintained at 30 °C with a glass-jacketed, thermostated cell. The needed volume of the nitric oxide stock solution was added through a gas-tight syringe by a Harvard Apparatus (South Natick, MA) Model 44 syringe pump. The needle tip was positioned just above the buffer solution. Unless noted otherwise, all sensor responses were measured in the presence of normal, ambient levels of oxygen in the buffer solution.

After the sensor was thermally equilibrated (1−2 min), the nitric oxide stock solution was injected into the buffer, while the CL signal was monitored continuously as a function of time. The resulting intensity versus time traces were stored for subsequent data analysis.

RESULTS AND DISCUSSION

Internal Solution pH. The pH of the internal solution is critical because both reactions involved in the detection of nitric oxide are pH sensitive. Kikuchi et al.[7] report the rapid formation of peroxynitrite from the oxidation of nitric oxide by hydrogen peroxide under neutral conditions. Under basic conditions, however, Blough and Zafiriou have concluded that the reaction does not proceed at an appreciable rate.[13] Under acidic conditions, peroxynitrite is thought to be formed but not directly from nitric oxide.[14] Evidence suggests that nitrosonium ion (NO^+) is formed initially from the acid-catalyzed reduction of nitric oxide. This nitrosonium ion subsequently reacts with hydrogen peroxide to form peroxynitrite.

From a thermodynamic standpoint, the formation of peroxynitrite from nitric oxide and hydrogen peroxide should be favorable with a Gibbs free energy of −15.5 kcal/mol. The overall reaction is

$$NO(g) + {}^3/_2H_2O_2(l) \rightarrow ONOOH(l) + H_2O(l) \qquad (1)$$

The Gibbs free energy of formation ($\Delta G_f°$) values for these various components are 20.69, −28.78, 18.7, and −56.69 kcal/mol for NO(g), H_2O_2(l), ONOOH(l), and H_2O(l), respectively.[15] The value for ONOOH has been estimated on the basis of the facts that

(8) Petriconi, G. L.; Papee, H. M. *Can. J. Chem.* **1966**, *44*, 977−980.
(9) Arnold, M. A.; Zhou, X.; Petsch, R. S. *Talanta* **1994**, *41* (5), 783−787.
(10) Doyle, M. P.; Hoekstra, J. W. *J. Inorg. Biochem.* **1981**, *14*, 351−358.
(11) Feelish, M. *J. Cardiovasc. Pharmacol.* **1991**, *17* (S3), 525−533.
(12) Feelish, M.; Noack, E. A. *Eur. J. Pharmacol.* **1987**, *139*, 19−30.
(13) Blough, N. V.; Zafiriou, O. C. *Inorg. Chem.* **1985**, *24*, 3502−3504.
(14) Laane, J.; Ohlsen, J. R. *Progr. Inorg. Chem.* **1980**, *27*, 469.
(15) Barrow, G. M. *Physical Chemistry*, 4th ed.; McGraw-Hill: New York, 1979.

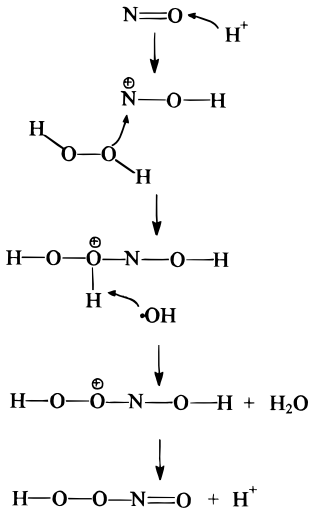

Figure 2. Proposed reaction mechanism for the formation of peroxynitrite from nitric oxide and hydrogen peroxide.

ONOOH(l) is about 38 kcal/mol more unstable than HNO_3(l),[16,19] and HNO_3(l) has a $\Delta G_f°$ of −19.31 kcal/mol.[15] More importantly, this reaction equilibrium should be independent of solution pH.

Clearly, the extent of reaction is pH dependent given reported observations in basic solutions.[13] Kinetics of the reaction must be responsible. In this regard, the individual reaction steps for the formation of peroxynitrite are not well understood. A similar reaction between hydrogen peroxide and nitrous acid, however, has been studied and a reaction sequence proposed.[17] By analogy, the NO−H_2O_2 reaction sequence might follow the steps outlined in Figure 2. The sequence begins with the proton activation of nitric oxide, followed by nucleophilic attack of the electropositive nitrogen by a lone pair of electrons from the oxygen in hydrogen peroxide. The resulting intermediate undergoes attack by a hydroxyl radical from the homolysis of hydrogen peroxide, thereby forming protonated peroxynitrous acid. Deprotonation results in the final product with regeneration of a proton. This mechanism is consistent with slow rates under basic conditions, as the initial activation step requires a proton.

In addition, quantum efficiency of the CL reaction between luminol and peroxynitrite is pH dependent, with larger efficiencies under more basic conditions. Another unwanted CL reaction is possible, however, if the pH is too high. For sensor operation, hydrogen peroxide and luminol must be present simultaneously in the internal solution. These two reagents can react in a CL manner under basic conditions. No CL reaction is observed, however, when the luminol level is less than 1 mM, the H_2O_2 level is less than 20 mM, and the internal solution pH is less than 9.0.

As expected, magnitude of the CL intensity, in response to nitric oxide, is strongly pH dependent. Figure 3 shows a series of CL intensity−time traces collected in 0.1 M pyrophosphate buffer at different solution pH values. The resulting pH profile is presented in the inset. A sharp profile is indicated with an optimum at 9.0. Lower quantum efficiencies are responsible for less response at lower pH, and slower formation of peroxynitrite reduces the response at higher pH.

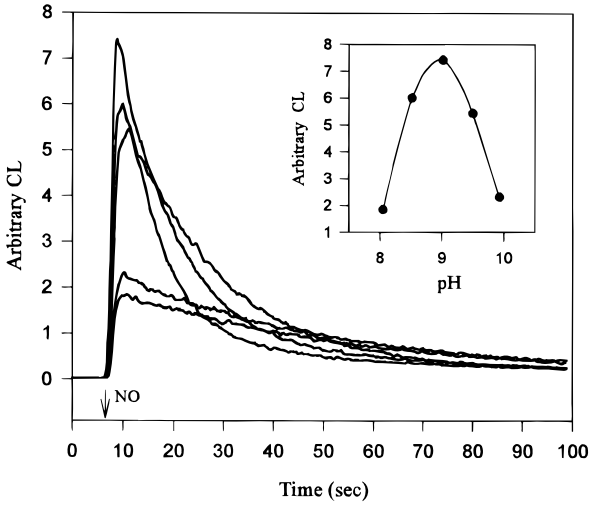

Figure 3. Effect of internal solution pH on sensor response when the buffer is 0.10 M pyrophosphate and the concentrations of luminol, hydrogen peroxide, and nitric oxide are 0.45 mM, 17.9 mM, and 80 μM, respectively. Inset shows the corresponding pH profile.

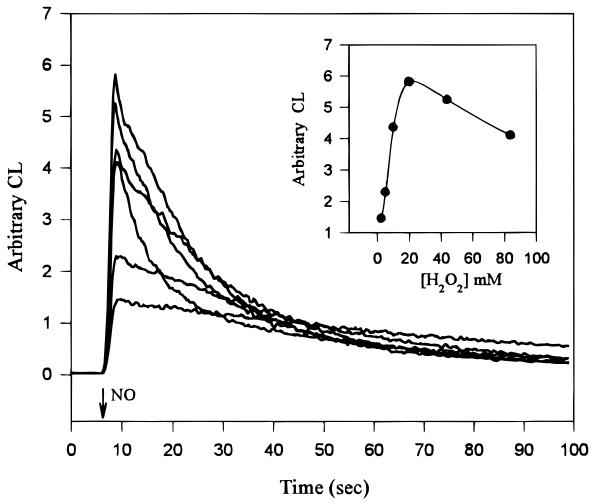

Figure 4. Effect of hydrogen peroxide level on sensor response when the buffer is pH 9.0, 0.5 M pyrophosphate and the concentrations of luminol and nitric oxide are 0.45 mM and 80 μM, respectively. Inset shows maximum CL signal as a function of hydrogen peroxide concentration.

Besides pyrophosphate, buffers of borate, bicarbonate, and glycine were tested. Borate is unsuitable due to the formation of peroxyborate[20] from the transperoxidation reaction between nitric oxide and borate. Elongated uprising signals were observed in borate buffers as nitric oxide was slowly released from the peroxyborate complex. Glycine buffers provided about half the magnitude of response obtained with pyrophosphate and bicarbonate buffers. Signals from pyrophosphate and bicarbonate buffers were similar.

Concentrations of Hydrogen Peroxide and Luminol. Optimum concentrations for both hydrogen peroxide and luminol have been identified for the internal solution. Intensity−time traces are shown in Figures 4 and 5 for different levels of hydrogen peroxide and luminol, respectively. For hydrogen peroxide, the largest signal is obtained with 20 mM hydrogen peroxide in a 0.05 M, pH 9.0 pyrophosphate buffer. Hydrogen peroxide levels between 19 and 25 mM were used for all sensors constructed

(16) McGrath, M. P.; Francl, M. M.; Rowland, F. S.; Hehre, W. J. *J. Phys. Chem.* **1988**, *92*, 5352−5357.
(17) Halfpenny, E.; Robinson, P. L. *J. Chem. Soc.* **1952**, 928−938.
(18) Pryor, W. A.; Church, D. F.; Govindan, C. K.; Crank, G. *J. Org. Chem.* **1982**, *47*, 156−159..
(19) Koppenol, W. H.; Moreno, J. J.; Pryor, W. A.; Ischiropoulos, H.; Beckman, J. S. *Chem. Res. Toxicol.* **1992**, *5*, 834−842.
(20) Keith, W. G.; Powell, R. E. *J. Chem. Soc. (A)* **1969**, 90.

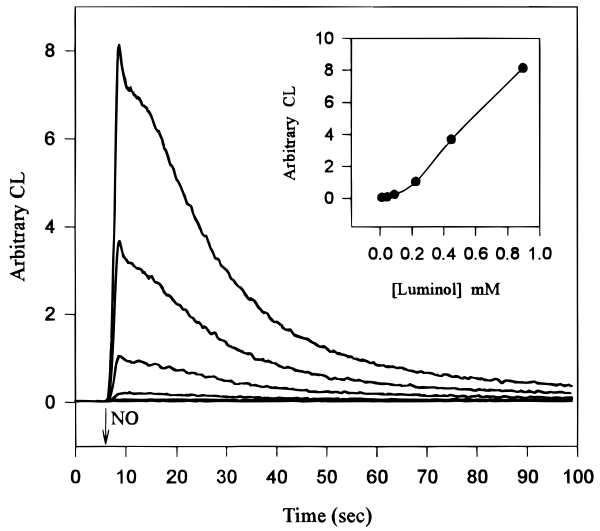

Figure 5. Effect of luminol level on sensor response when the buffer is pH 9.0, 0.5 M pyrophosphate and the concentrations of hydrogen peroxide and nitric oxide are 20.5 mM and 80 μM, respectively. Inset shows the corresponding luminol profile.

with pyrophosphate buffer. The best concentration of hydrogen peroxide is slightly greater when a bicarbonate buffer is used. Levels between 20 and 43 mM give the highest responses in bicarbonate buffers.

The Figure 4 inset shows the hydrogen peroxide concentration profile, which reveals a steep increase in response up to 20 mM, followed by a more gradual decline at higher hydrogen peroxide levels. This decline is likely due to the fluorescence quenching characteristics of hydrogen peroxide.[21]

In contrast, the response continually increases as a function of luminol concentration (see Figure 5 inset). The practical upper limit for luminol is reached at 1.3 mM when the background CL from the reaction with hydrogen peroxide becomes evident. The concentration of luminol was between 0.8 and 1.0 mM in all subsequent experiments.

Selection of Sensor Membrane. The gas-permeable membrane is needed to separate the detection reagents in the internal solution from the sample solution. This membrane should freely pass nitric oxide while isolating the sample and internal solutions in terms of nonvolatile species. Membranes of microporous Teflon, nonmicroporous Teflon (Tefzel), silicone, and polycarbonate were tested for their ability to pass nitric oxide. Typical intensity−time traces collected from sensors built with these various membranes are presented in Figure 6 for comparison. Only the silicone membrane permitted sufficient permeability of nitric oxide for sensor operation. Based on these results, all sensors were constructed with nonvulcanized matte-matte silicone sheetings. Unless noted otherwise, all membranes had a thickness of 0.051 mm.

The intensity−time trace shown in Figure 6 for the silicone membrane illustrates the time-dependent response of this type of sensor to a step-change in nitric oxide concentration. Initially, a steep increase in intensity is observed, followed by a decay toward the background signal. A mathematical model has been derived to explain this type of response.

Modeling of the Response Mechanism. The concentration of nitric oxide decreases continuously during the sensor response

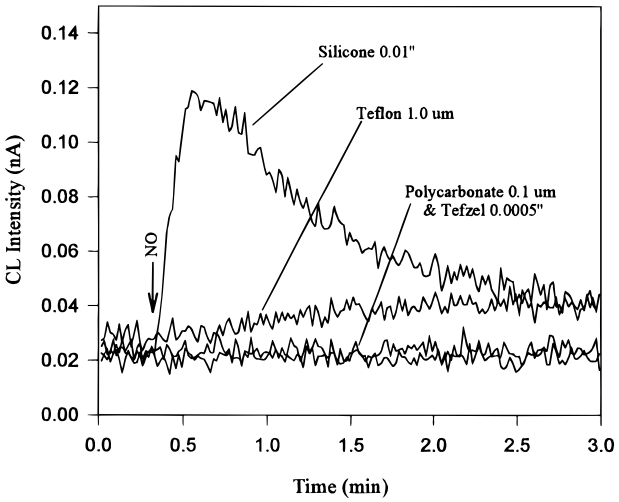

Figure 6. Responses from sensors constructed with membranes composed of silicone, microporous Teflon, polycarbonate, and Tefzel.

due to the oxidation of nitric oxide by ambient oxygen. The reduction in nitric oxide accounts for the decline in sensor response with time. A model can be used to relate the initial nitric oxide concentration in the sample and the resulting sensor response.

This model is based on a response mechanism shown schematically as follows:

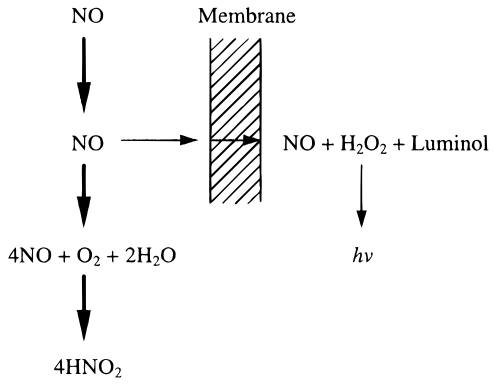

In this model, nitric oxide either crosses the membrane for detection or reacts with ambient oxygen. A larger fraction of nitric oxide is lost by oxidation.

In the presence of oxygen, nitric oxide is readily oxidized to NO_x, especially NO_2 or HNO_2.[22,23] In aqueous solution, according to Wink,[22] nitric oxide undergoes the following reaction with oxygen:

$$4NO(aq) + O_2(aq) + 2H_2O(aq) \rightarrow 4HNO_2(aq) \quad (2)$$

The reaction rate is second order with respect to nitric oxide and first order with respect to oxygen, with a rate constant of 6.0 ($\pm$1.5) $\times$ 10^6 M^{-2} s^{-1} in pH 7.4, 0.001 M phosphate buffer at 22 °C. The total rate of nitric oxide consumption equals the sum of the individual rates corresponding to oxidation, diffusion across the membrane, and any other means (i.e., consumption by trace

(21) Cavatorta, P.; Favilla, R.; Mazzini, A. *Biochim. Biophys. Acta* **1979**, *578*, 541−546.

(22) Wink, D. A.; Darbyshire, J. F.; Nims, R. W.; Saavedra, J. E.; Ford, P. C. *Chem. Res. Toxicol.* **1993**, *6*, 23−27.

(23) Olbregts, J. *Int. J. Chem. Kinet.* **1985**, *17*, 835−848.

contaminates and escape from the surface). Hence,

$$-\left.\frac{\mathrm{d[NO]}}{\mathrm{d}t}\right|_{\text{total}} = \left(-\left.\frac{\mathrm{d[NO]}}{\mathrm{d}t}\right|_{\mathrm{O_2}}\right) + \left(-\left.\frac{\mathrm{d[NO]}}{\mathrm{d}t}\right|_{\text{memb}}\right) + \left(-\left.\frac{\mathrm{d[NO]}}{\mathrm{d}t}\right|_{\text{other}}\right) \quad (3)$$

where the terms correspond to oxidation, diffusion across the membrane, and all other processes, respectively. Assuming that consumption by oxidation dominates,

$$-\left.\frac{\mathrm{d[NO]}}{\mathrm{d}t}\right|_{\text{memb}} \cong 0 \quad (4)$$

$$-\left.\frac{\mathrm{d[NO]}}{\mathrm{d}t}\right|_{\text{other}} \cong 0 \quad (5)$$

then

$$-\left.\frac{\mathrm{d[NO]}}{\mathrm{d}t}\right|_{\text{total}} = -\left.\frac{\mathrm{d[NO]}}{\mathrm{d}t}\right|_{\mathrm{O_2}} = -\frac{\mathrm{d[NO]}}{\mathrm{d}t}$$

or

$$-\frac{\mathrm{d[NO]}}{\mathrm{d}t} = k[\mathrm{NO}]^2[\mathrm{O_2}] \quad (6)$$

$$\int_{[\mathrm{NO}]_0}^{[\mathrm{NO}]} -\frac{\mathrm{d[NO]}}{[\mathrm{NO}]^2} = \int_{t=0}^{t} k[\mathrm{O_2}]\,\mathrm{d}t \quad (7)$$

If the ambient oxygen level is relatively constant, then

$$[\mathrm{NO}] = \frac{1}{1/[\mathrm{NO}]_0 + k[\mathrm{O_2}]t} \quad (8)$$

where $[\mathrm{NO}]_0$ and [NO] correspond to the concentrations of nitric oxide at times zero and t, respectively. This assumption is generally valid because the ambient oxygen level is 0.2 mM, which is several times larger than initial nitric oxide concentrations. Equation 8 indicates that [NO] decreases with time.

At the same time, some nitric oxide molecules cross the silicone membrane and this diffusion process should obey Fick's first and second laws:

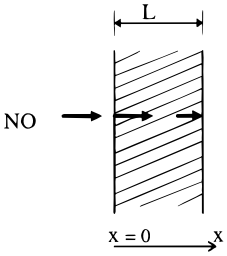

$$J = -D\frac{\partial C(x,t)}{\partial X} \quad (9)$$

$$\frac{\partial C(x,t)}{\partial t} = D\frac{\partial^2 C(x,t)}{\partial X^2} \quad (10)$$

Boundary conditions are determined from eq 8 for nitric oxide concentrations at the outer surface of the membrane ($x = 0$). The concentration of nitric oxide at the inner surface ($x = L$) is set at zero, which assumes the rates of reaction in the internal solution are not rate limiting. The boundary conditions (BC) are

$$C(0,t) = 1/(a + bt)$$

$$C(L,t) = 0 \qquad 0 < t < \infty$$

where $a = 1/[\mathrm{NO}]_0$, $b = k[\mathrm{O_2}]$, and $C(0,t)$ is given by eq 8.

For initial conditions (IC), the nitric oxide concentration is set at zero across the membrane:

$$C(x,0) = 0 \qquad 0 < x < \mathrm{L}$$

According to Farlow,[24] the above partial differential equation (PDE) with nonzero boundary conditions can be converted to a partial differential equation with homogeneous boundary conditions by the following procedure:

let
$$S(x,t) = \frac{1}{a + bt}\left(1 - \frac{x}{L}\right) \quad (11)$$

$$C(x,t) = S(x,t) + U(x,t) \quad (12)$$

where $S(x,t)$ and $U(x,t)$ are the steady-state and transient components, respectively. The previous problem can be transferred into the following:

$$\begin{array}{ll} \text{PDE} & U_t = DU_{xx} - S_t \\ \text{BC} & U(x,0) = 0 \\ & U(x,L) = 0 \\ \text{IC} & U(x,0) = \frac{1}{a}\left(1 - \frac{x}{L}\right) \end{array} \quad (13)$$

which can be solved with eigenfunction expansions.[24] The resulting concentration profile is

$$C(x,t) = \frac{1}{a + bt}\left(1 - \frac{x}{L}\right) + \sum_{n=1}^{\infty} a_n \sin\left(\frac{n\pi x}{L}\right) \exp\left[-\left(\frac{n\pi\alpha}{L}\right)^2 t\right] + \sum_{n=1}^{\infty} \sin\left(\frac{n\pi x}{L}\right) \int_0^t f_n(t) \exp\left[-\left(\frac{n\pi\alpha}{L}\right)^2 (t - \tau)\right] \mathrm{d}\tau \quad (14)$$

where $a_n = -2/an\pi$, $\alpha = D^{0.5}$, and

$$f_n(t) = \frac{2b}{n\pi(a + bt)^2}$$

The concentration gradient at $x = L$ is

$$\frac{\partial}{\partial x}C(L,t) = \frac{-1}{(a + bt)L} - \sum_{j=1}^{\infty} \frac{2}{aL} \cos(j\pi) \exp\left[-\left(\frac{\alpha j\pi}{L}\right)^2 t\right] + \sum_{j=1}^{\infty} \frac{2b}{L} \cos(j\pi) \int_0^t \frac{1}{(a + b\tau)^2} \exp\left[-\left(\frac{\alpha j\pi}{L}\right)^2 (t - \tau)\right] \mathrm{d}\tau \quad (15)$$

So the flux of nitric oxide at $x = L$, just inside the membrane,

(24) Farlow, S. J. *Partial Differential Equations for Scientists & Engineers*; John Wiley & Sons, Inc.: New York, 1982; pp 44− 70.

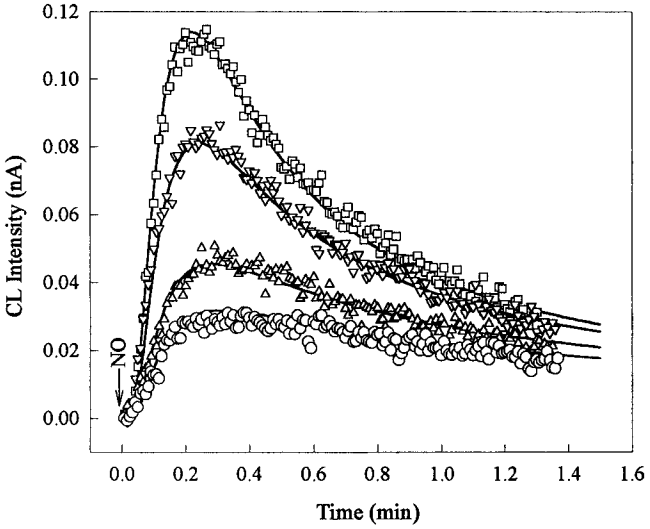

Figure 7. Measured (symbols) and predicted (solid lines) sensor responses for initial nitric oxide levels of 7.9 (O), 12.0 (△), 25.0 (▽), and 39.9 (□) μM.

would be

$$\text{flux} = -D\frac{\partial}{\partial x}C(L,t) \qquad (16)$$

and the CL intensity (In) should be linearly related to this flux:

$$\text{In} = A \times \text{flux} \qquad (17)$$

where A is a proportionality constant.

Validity of the model has been tested by superimposing the predicted time-dependent response with actual intensity−time traces. Figure 7 shows examples of such traces for different nitric oxide concentrations. The fit is excellent. These predictions required fitting the model expression to actual sensor responses by adjusting the rate constant for the oxidation reaction (k) and the diffusion coefficient for nitric oxide through the silicone membrane (D). Thickness of the membrane was set at 0.051 mm. The proportionality constant between the measured intensity and computed nitric oxide flux was obtained by dividing the current measured at the peak response for 39.9 μM nitric oxide by the computed flux at the corresponding reaction time. This proportionality constant was used for all subsequent values.

Fitted values for k and D can be examined to further substantiate model validity. The best prediction results are obtained when $k = 9.5(\pm 0.5) \times 10^6$ M^{-2} s^{-1} and $D = 5.0(\pm 0.2) \times 10^{-11}$ m^2 s^{-1}. Others have measured the oxidation rate constant under similar reaction conditions.[22] At 22 °C in a 0.001 M, pH 7.4 phosphate buffer, $k = 6(\pm 1.5) \times 10^6$ M^{-2} s^{-1}, which is slightly below our value, which was measured at 30 °C in a 0.1 M, pH 9.0 pyrophosphate buffer. The closeness of these values is significant and helps validate the model.

In terms of the diffusion coefficient, literature values are not available for the specific polymer used in this experiment. Nevertheless, the validity of our fitted value for the diffusion coefficient can be established by comparing predicted and measured response times in the absence of oxygen for sensors with a specific membrane thickness.

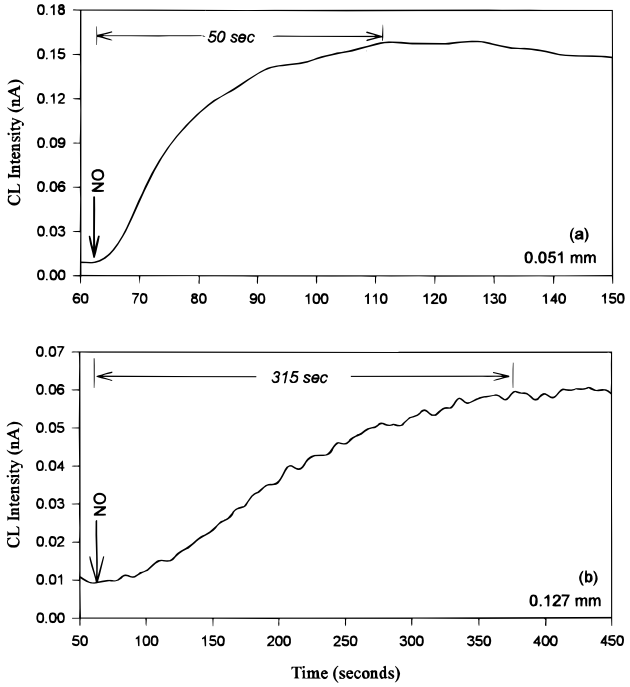

Figure 8. Responses to 77.4 μM nitric oxide in the absence of oxygen for sensors constructed with silicone membranes with thicknesses of 0.051 (a) and 0.127 mm (b).

For a random walk process,[25] the distance a molecule moves during a certain time (t) can be calculated as $\delta = (Dt)^{0.5}$. In the case of diffusion of nitric oxide inside the silicone layer, the time (t_1) can be calculated for nitric oxide to traverse the distance δ ($t_1 = \delta 2/D$). This time should equal the sensor response time when δ equals the membrane thickness and no oxygen is present in the sample solution. If D is $5.0(\pm 0.2) \times 10^{-11}$ m^2 s^{-1}, t_1 would be 51.6 ± 2.0 and 322.6 ± 12.4 s for membrane thicknesses of 0.051 and 0.127 mm, respectively. Figure 8 shows intensity−time traces for sensors with these membrane thicknesses. Although the exact response time is difficult to access, the response appears to reach steady state in 50 s for the thinner membrane and 315 s for the thicker membrane. The excellent agreement between predicted and measured response times validates the diffusion coefficient obtained from this model.

Sensor Response Properties. Maximum sensor responses were achieved between 10 and 17 s following addition of nitric oxide to a stirred volume of the external buffer. This external solution was a 0.05 M, pH 7.4 phosphate buffer containing normal ambient levels of oxygen and maintained at 30 °C. Typical sensor outputs are presented in Figure 7. Calibration curves were constructed by plotting the maximum peak height relative to the initial nitric oxide concentration in the sample. The dynamic range extends from 5 to 40 μM nitric oxide, with a computed limit of detection (S/N = 3) of 1.3 μM. Values predicted from our model compare favorably with measured values for all concentrations tested. Predicted values are within the 95% confidence interval of the corresponding measured values.

One concern with this type of sensor is the consumption of reagents in the internal solution and the corresponding changes in sensor output. This issue is particularly significant given the relatively sharp pH and concentration profiles for the internal

(25) Bard, A. J.; Faulkner, L. R. *Electrochemical Methods Fundamentals and Applications*; John Wiley & Sons, Inc.: New York, 1980; p 129.

solution (see insets of Figures 4−6). No changes in sensor output were noted for seven repeated measurements of the same sample. Typical relative standard deviations were 5.5% for such repeated measurements. Theoretically, the internal solution can last over 100 h when the sensor is used continuously to measure 40 μM nitric oxide, because only a small amount of nitric oxide (about 0.3% of total luminol in the internal solution) crosses the membrane during this time period. The stock internal solution remained unchanged for more than 2 weeks when stored in a sealed glass bottle at room temperature. In addition, diffusion properties across the membrane were stable. One membrane was used continuously for a 3-month period without any noticeable sign of deterioration or change in sensor response rate.

Selectivity is a major issue for nitric oxide measurements in biological systems. Several compounds have been tested as potential interferences. In each case, the potential interference was added to the buffer solution before addition of nitric oxide. Responses recorded with and without the interfering species were then compared for three replicate experiments. The mean response to 61.2 μM nitric oxide was set to 100%, and all subsequent responses were judged relative to this value. Mean (±standard deviation) responses for the blank and in the presence of 25.0 mM bicarbonate, 0.1 mM ammonia, 1.0 mM dopamine, 5.1 mM uric acid, 3.0 mM ascorbic acid, and 3.8 mM L-cysteine were 100.0 ± 5.1, 97.8 ± 9.8, 97.8 ± 7.4, 121.0 ± 11.0, 118.0 ± 16.0, 126.0 ± 15.0, and 65.0 ± 12.0%, respectively.

Carbon dioxide and ammonia were tested as examples of acidic and basic gases that might influence sensor response by affecting the pH of the internal solution. No differences in response were noted in the presence of either carbon dioxide or ammonia.

All other tested compounds influence the measurement. Dopamine, uric acid, and ascorbic acid are positive interferences, and cysteine is a negative interference. Interference from the first three species is caused by consumption of ambient oxygen due to the oxidation of these compounds. The resulting lower oxygen level slows the oxidation of nitric oxide, which results in a larger peak response. Interference from cysteine, on the other hand, is caused by a reduction in nitric oxide concentration due to reaction with the thiol group on this amino acid.[18] It must be noted that none of these tested compounds interferes with the sensor operation; only the levels of nitric oxide and oxygen in the sample.

CONCLUSIONS

The nitric oxide sensor described in this paper is capable of detecting micromolar levels of nitric oxide in aqueous matrixes under physiological conditions of temperature and pH. The mathematical model derived in this work can accurately predict sensor response by accounting for the relative rates of oxidation and detection. This model is not limited to the CL sensor demonstrated here but is applicable to essentially all nitric oxide sensor designs. Results indicate that the rapid loss of nitric oxide in the sample solution is significant on the time scale of the sensor response, and this loss of analyte greatly complicates the analytical measurement. Selectivity of this CL sensor is excellent in terms of a lack of direct sensor response to other components. Nevertheless, systematic errors are noted in the presence of oxidizable species that can react with and thereby decrease the endogenous concentrations of oxygen.

Received for review December 19, 1995. Accepted March 2, 1996.[⊗]

AC951224G

[⊗] Abstract published in *Advance ACS Abstracts,* April 15, 1996.